

Studies of the Formation and Decomposition Pathways for Cationic Zirconocene Hydrido Silyl Complexes

Vladimir K. Dioumaev and John F. Harrod^{*,†}

Chemistry Department, McGill University, Montreal, Quebec, Canada H3A 2K6

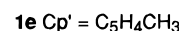
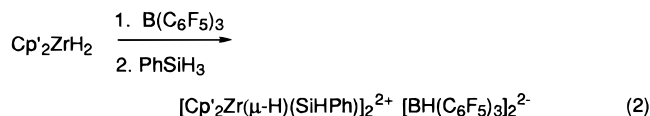
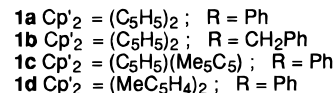
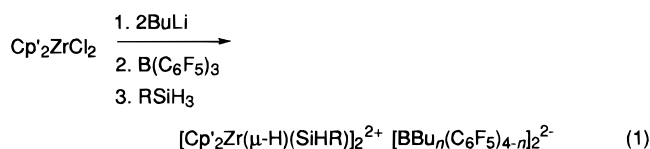
Received October 21, 1996[®]

Reactions and intermediates leading to zirconocene complexes $[\text{Cp}'_2\text{Zr}(\mu\text{-H})(\text{SiHR})]_2^{2+}[\text{BR}'_n(\text{C}_6\text{F}_5)_{4-n}]_2^{2-}$ ($\text{Cp}' = \text{Cp}, \text{MeCp}, \text{Me}_5\text{Cp}$; $\text{R} = \text{Ph}, \text{PhCH}_2$; $\text{R}' = \text{Bu}$ or H ; **1a–e**) were investigated *in situ* by NMR and EPR studies and by trapping unstable intermediates with PMe_3 . Two novel Zr^{III} complexes, $[\text{Cp}_2\text{Zr}^{\text{III}}]^+[\text{BBu}_n(\text{C}_6\text{F}_5)_{4-n}]^-$ (**5**) and $[\text{Cp}_2\text{Zr}^{\text{III}}(\text{PMe}_3)_2]^+[\text{BBu}_n(\text{C}_6\text{F}_5)_{4-n}]^-$ (**8**) were identified by EPR spectroscopy. Redistribution of borate butyl and pentafluorophenyl ligands was found to occur by a direct boron to boron migration and not by a metal-assisted mechanism. The latter was ruled out by an independent synthesis of expected reaction intermediates for both reaction pathways ($[\text{Ph}_3\text{C}][\text{BBu}(\text{C}_6\text{F}_5)_3]$, $[\text{Cp}_2\text{Zr}(\text{C}_6\text{F}_5)]^+[\text{BBu}_n(\text{C}_6\text{F}_5)_{4-n}]^-$, and $[\text{Cp}_2\text{Zr}(\text{C}_6\text{F}_5)(\mu_3\text{-HB}(\text{C}_6\text{F}_5)_3)]_2$) and an investigation of their model redistribution reactions by NMR spectroscopy.

Introduction

Coordination catalysts for silane polymerization are currently of scientific and technological interest because silicon-containing polymers have significant potential as materials for ceramic precursors for electronics and integrated optics.^{1–6} Transition-metal catalysts offer an unprecedented control over the stereochemistry of the polymeric products and the cyclic/linear chain selectivity.^{7–10} On the other hand, there is still room for improvement in the catalyst design to produce polysilanes with molecular chains long enough to ensure good mechanical properties. Most of the progress in this field is based on studies of the reaction intermediates and mechanisms involving neutral Cp_2MR_2 ($\text{M} = \text{Ti}, \text{Zr}, \text{Hf}$, $\text{R} = \text{alkyl}, \text{H}, \text{silyl}$) compounds.^{10–15} We recently reported a novel type of cationic catalyst for the dehydrocoupling of primary silanes, which proved to have certain advantages over neutral analogs.^{16,17} The un-

usual structure of the species isolated from the reaction mixture, **1** (eqs 1 and 2),¹⁸ prompted us to investigate



the chemistry of this system more thoroughly. We now report studies of the formation pathways and reactivity of the reaction products in solution using multinuclear, multidimensional NMR spectroscopy and EPR spectroscopy.

Results and Discussion

I. Formation Pathway for 1. Mixtures of neutral Cp_2MX_2 metallocenes ($\text{M} = \text{Ti}, \text{Zr}, \text{Hf}$; $\text{X} = \text{Me}, \text{H}$) and primary silanes were studied earlier, and analogs of compounds **1** were isolated from them.^{12,19–22} However,

(16) Dioumaev, V. K.; Harrod, J. F. *Organometallics* **1994**, *13*, 1548–1550.

(17) Dioumaev, V. K.; Harrod, J. F. *J. Organomet. Chem.* **1996**, *521*, 133–143.

(18) Dioumaev, V. K.; Harrod, J. F. *Organometallics* **1996**, *15*, 3859–3867.

(19) Aitken, C.; Harrod, J. F.; Samuel, E. *Can. J. Chem.* **1986**, *64*, 1677–1679.

(20) Mu, Y.; Aitken, C.; Cote, B.; Harrod, J. F.; Samuel, E. *Can. J. Chem.* **1991**, *69*, 264–276.

(21) Takahashi, T.; Hasegawa, M.; Suzuki, N.; Saburi, M.; Rousset, C. J.; Fanwick, P. E.; Negishi, E. *J. Am. Chem. Soc.* **1991**, *113*, 8564–8566.

[†] E-mail: Harrod@omc.lan.McGill.ca.

[®] Abstract published in *Advance ACS Abstracts*, May 15, 1997.

(1) *Inorganic and Organometallic Polymers*; Zeldin, M., Wynne, K. J., Allcock, H. R., Eds.; American Chemical Society: Washington, DC, 1988.

(2) Mark, J. E.; Alcock, H. R.; West, R. C. *Inorganic Polymers*; Prentice-Hall: Englewood Cliffs, NJ, 1992; pp 186–236.

(3) *Silicon-Based Polymer Science: A Comprehensive Resource*; Ziegler, J. M., Fearon, F. W. G., Eds.; American Chemical Society: Washington, DC, 1990.

(4) West, R. *J. Organomet. Chem.* **1986**, *300*, 327–346.

(5) Miller, R. D.; Michl, J. *Chem. Rev.* **1989**, *89*, 1359–1410.

(6) Ziegler, J. M. *Mol. Cryst. Liq. Cryst.* **1990**, *190*, 265–282.

(7) Gauvin, F.; Harrod, J. F. *Can. J. Chem.* **1990**, *68*, 1638–1640.

(8) Banovetz, J. P.; Stein, K. M.; Waymouth, R. M. *Organometallics* **1991**, *10*, 3430–3432.

(9) Harrod, J. F. In *Inorganic and Organometallic Polymers with Special Properties*; Laine, R. M., Ed.; Kluwer Academic: Dordrecht, The Netherlands, 1992; Vol. 206, pp 87–98.

(10) Tilley, T. D. *Acc. Chem. Res.* **1993**, *26*, 22–29.

(11) Samuel, E.; Harrod, J. F. *J. Am. Chem. Soc.* **1984**, *106*, 1859–1860.

(12) Aitken, C. T.; Harrod, J. F.; Samuel, E. *J. Am. Chem. Soc.* **1986**, *108*, 4059–4066.

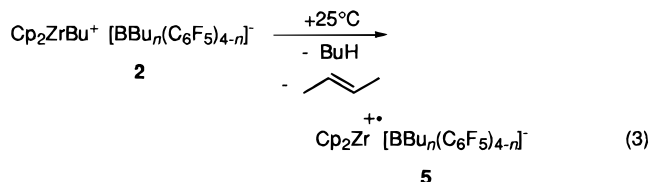
(13) Harrod, J. F. In *Inorganic and Organometallic Polymers*; Zeldin, M., Wynne, K. J., Allcock, H. R., Eds.; American Chemical Society: Washington, DC, 1988; pp 89–100.

(14) Woo, H.-G.; Tilley, T. D. *J. Am. Chem. Soc.* **1989**, *111*, 3757–3758.

(15) Woo, H.-G.; Tilley, T. D. *J. Am. Chem. Soc.* **1989**, *111*, 8043–8044.

Further, the high value for g_y indicates the presence of a strong π -donor ligand in the bisectorial plane of the sandwich.²⁸ Indeed, in group 4 $\text{Cp}_2\text{M}^{\text{III}}\text{X}$ complexes g_y primarily depends on the HOMO–LUMO ($1a_1 \rightarrow b_2$) energy gap, where the HOMO, nonbonding $1a_1$, is largely d_z^2 (in the Dahl–Petersen coordination system) and is fairly insensitive to the σ -donor properties of X. On the other hand, the LUMO, b_2 , is mainly d_{xz} and acts as a π -acceptor. Hence, the energy gap is governed by the π -donor ability of the X ligand.²⁸ In the case of **5** there is no directly attached ligand X and such a π -donation can only be the result of a tight contact with the solvent, counterion, or a Cp of another metallocene. Given the ability of such ionic compounds to form liquid clathrates (or solvent-separated ion pairs),^{18,29} a tight contact with the toluene solvent is the most likely explanation. It also accounts for the discrepancies in the $g_{\text{av}}/g_{\text{iso}}$ values.

Compound **5** could, in principle, also be synthesized by reaction of Cp_2ZrBu and $[\text{Ph}_3\text{C}]^+[\text{BBu}_n(\text{C}_6\text{F}_5)_{4-n}]^-$. Unfortunately, the trityl cation is reduced by the Zr(III) compounds and the major EPR-active product in this case is Ph_3C^* ($g = 2.0021$, m). Alternatively, thermal (+25 °C) decomposition of **2** gives **5** (eq 3),



which is formed at the expense of two less stable compounds. These can be detected in the early stages of decomposition ($g = 1.9964$, s, $a(\text{Zr}) = 7.1$ G and $g = 1.9860$, s, $a(\text{Zr}) = 25.8$ G; parts a and b of Figure 2). The compound with $g = 1.9964$ is also formed during photolysis of **1a** (*vide infra*). It is even more electron-deficient than **5** and can be tentatively assigned to the tight ion pair form of **5**, which has a cation–anion interaction but no strongly coordinated solvent. Due to the interference of the second unidentified compound, this assignment could not be confirmed by the frozen-glass EPR spectrum. However, such a coordination of fluorophenylborates has been previously reported to occur either through F atoms^{26,30,31} or through another ligand of the borate anion, $[\text{BR}(\text{C}_6\text{F}_5)_3]^-$ ($\text{R} = \text{Me}$,^{31–37} CH_2Ph ^{38–40}).

(28) Lukens, J.; Smith, W. W., III; M. R.; Andersen, R. A. *J. Am. Chem. Soc.* **1996**, *118*, 1719–1728.

(29) Atwood, J. L. In *Coordination Chemistry of Aluminum*; Robinson, G. H., Ed.; VCH: New York, 1993; pp 197–232.

(30) Yang, X.; Stern, C. L.; Marks, T. J. *Organometallics* **1991**, *10*, 840–842.

(31) Yang, X.; Stern, C. L.; Marks, T. J. *J. Am. Chem. Soc.* **1994**, *116*, 10015–10031.

(32) Yang, X.; Stern, C. L.; Marks, T. J. *J. Am. Chem. Soc.* **1991**, *113*, 3623–3625.

(33) Deck, P. A.; Marks, T. J. *J. Am. Chem. Soc.* **1995**, *117*, 6128–6129.

(34) Giardello, M. A.; Eisen, M. S.; Stern, C. L.; Marks, T. J. *J. Am. Chem. Soc.* **1995**, *117*, 12114–12129.

(35) Bochmann, M.; Lancaster, S. J.; Hursthouse, M. B.; Malik, K. M. A. *Organometallics* **1994**, *13*, 2235–2243.

(36) Gomez, R.; Green, M. L. H.; Haggitt, J. L. *J. Chem. Soc., Chem. Commun.* **1994**, 2607–2608.

(37) Gillis, D. J.; Tudoret, M.-J.; Baird, M. C. *J. Am. Chem. Soc.* **1993**, *115*, 2543–2545.

(38) Pellecchia, C.; Grassi, A.; Immirzi, A. *J. Am. Chem. Soc.* **1993**, *115*, 1160–1162.

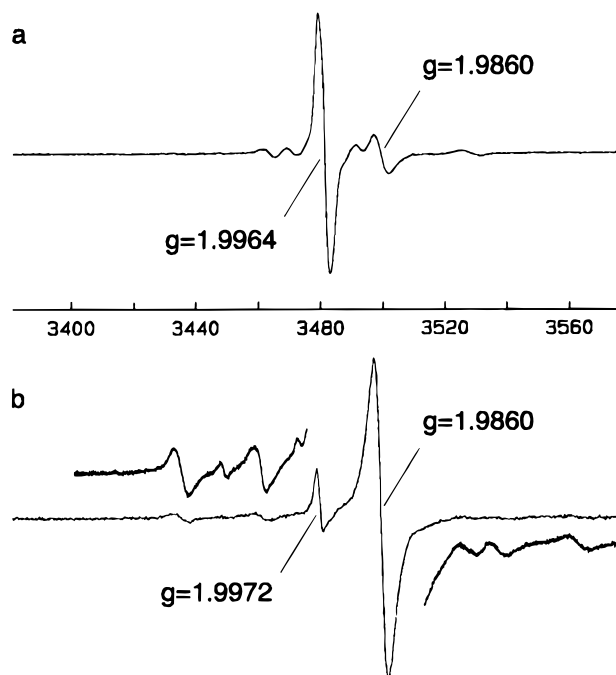


Figure 2. EPR spectra of the thermal decomposition products of **2** in toluene: (a) main peak tentatively assigned to $[\text{Cp}_2\text{Zr}]^+[\text{BBu}_n(\text{C}_6\text{F}_5)_{4-n}]^-$; (b) the peak at 1.9972 tentatively assigned to crotylzirconocene.

Compound **5** readily abstracts hydrogen from PhSiH_3 , leading to the same product **4** as the low-temperature path. The rest of the steps are the same for both temperatures. The obvious difference between the low- and room-temperature synthesis and the key to the catalytic performance is the presence of low-oxidation-state compound **5** in the latter. If silane is in excess, the room-temperature synthesis furnishes **1a** as the final product only when all PhSiH_3 is consumed. Addition of a fresh portion of silane does not reinitiate the dehydrocoupling reaction. It is thus clear that production of **1a** is a sterile branch of the catalytic cycle. When the reaction is still in progress, **6** is consumed in a productive cycle fast enough to preclude irreversible formation of its dimer **1a**. The poor performance of the $\text{Cp}_2\text{ZrMe}_2/\text{B}(\text{C}_6\text{F}_5)_3$ catalyst resides in its failure to produce Zr(III).

Further support for the structure of **5** was provided by trapping it with PMe_3 . The product, **8**, can be readily identified by EPR spectroscopy ($g = 1.9877$, t; $a(\text{P}) = 33.0$ G, $a(\text{Zr}) = 23.4$ G; Figure 3). The multiplicity of the signal and the value of $a(\text{P})$ clearly indicate a bis(phosphine) adduct, $\text{Cp}_2\text{ZrX}(\text{PMe}_3)_2$, while the lack of any observable hyperfine coupling to X (band width <3 G) and the presence of borate anion (^1H NMR spectroscopy) suggest that “substituent X” is a positive charge, which is in good agreement with the electron count for **8**. Indeed, if X is a two-electron-donor ligand, $\text{Cp}_2\text{ZrX}(\text{PMe}_3)_2$ is a 19e complex, whereas a zero-electron donor (positive charge) gives a more reasonable 17e configuration and more space to accommodate two phosphines. Complex **8** was independently synthesized by oxidation of $\text{Cp}_2\text{Zr}^{\text{II}}(\text{PMe}_3)_2$ with $[\text{Ph}_3\text{C}]^+[\text{BBu}_n(\text{C}_6\text{F}_5)_{4-n}]^-$ (eq 4). To the best of our knowledge there is only one other

(39) Pellecchia, C.; Immirzi, A.; Grassi, A.; Zambelli, A. *Organometallics* **1993**, *12*, 4473–4478.

(40) Pellecchia, C.; Grassi, A.; Zambelli, A. *Organometallics* **1994**, *13*, 298–302.

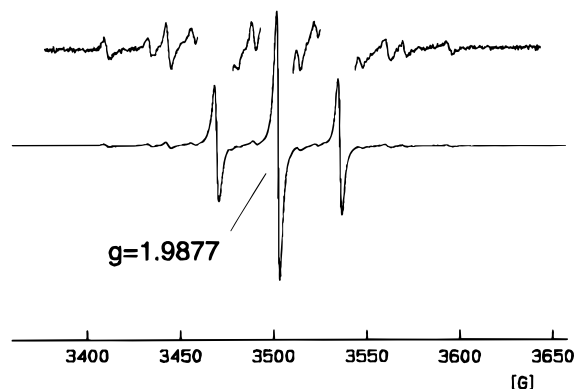
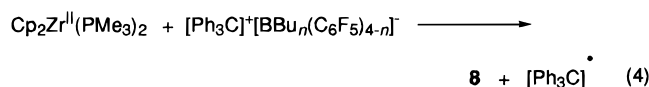


Figure 3. EPR spectrum of $[\text{Cp}_2\text{Zr}(\text{PMe}_3)_2]^+[\text{BBu}_n(\text{C}_6\text{F}_5)_{4-n}]^-$ in C_6D_6 .

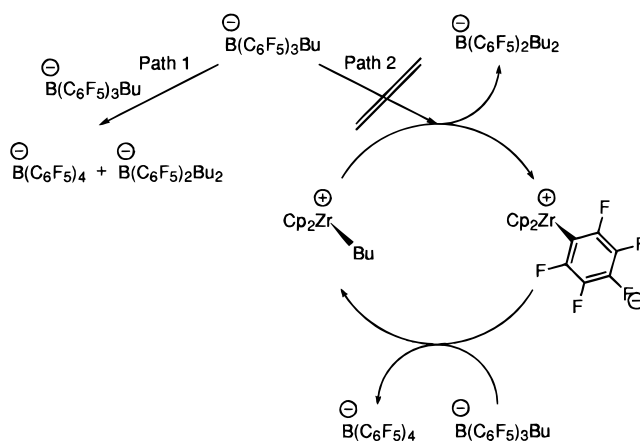
reported example of a stable zirconocene(III) cation radical in the condensed phase $(\text{Me}_3\text{SiCp})_2\text{Zr}^{\text{III}}(\text{dmp})^+\text{BF}_4^-$: $g = 1.9871$, $a(\text{P}) = 26.5$ G,⁴¹ although titanocene analogs $(\text{Cp}_2\text{Ti}^{\text{III}}(\text{L})_2)^+$, $\text{L} = \text{PMe}_3$, THF, MeCN, $\text{H}_2\text{NCH}_2\text{CH}_2\text{NH}_2$, $\text{Me}_2\text{NCH}_2\text{CH}_2\text{NMe}_2$, 2,2-bipyridyl) are well-known.^{42–47}



II. Ligand Redistribution. The chemistry of the borate counterion has so far been neglected in the discussion. However, the structure and reactivity of the borate anion proved to be more complicated than originally expected. Indeed, a number of anions with a general formula $[\text{BBu}_n(\text{C}_6\text{F}_5)_{4-n}]^-$ are actually formed (as observed by ^{19}F NMR) instead of a single monobutylborate. In view of the large number of publications involving $\text{B}(\text{C}_6\text{F}_5)_3$ and $[\text{BR}(\text{C}_6\text{F}_5)_3]^-$ it is surprising that there are no reported precedents for this type of redistribution.

Boron ligand redistribution is likely to occur by one of two mechanisms. It either can occur by a direct boron to boron migration (Scheme 2, path 1) or can be metal-assisted (Scheme 2, path 2). Tetrahaloborates were reported to participate in ligand exchange via dissociation, followed by an $\text{S}_{\text{N}}2$ attack of the halide on another borate molecule.⁴⁸ Such a dissociation step is less likely to occur in the case of $[\text{BBu}_n(\text{C}_6\text{F}_5)_{4-n}]^-$, as neither Bu nor C_6F_5 is a good leaving group, but it cannot be completely excluded. To the best of our knowledge, no alkyl or aryl boron to boron bridges or ligand redistributions have ever been reported, while boron to metal ligand transfer reactions^{31,36,49–55} and bridging struc-

Scheme 2. Ligand Redistribution Pathways for $[\text{BPh}^F_n\text{Bu}_{4-n}]^-$ Anions



tures^{31–33,35} are well-known. If the ligand redistribution follows the metal-assisted path, there should be a reversible formation of $\text{Cp}_2\text{Zr}(\text{C}_6\text{F}_5)^+$. To probe the feasibility of this path, the synthesis of cationic $\text{Cp}_2\text{Zr}(\text{C}_6\text{F}_5)(\mu\text{-H})_2$ (Scheme 3). A rapid reaction occurred, but the complex $[\text{Cp}_2\text{Zr}(\text{C}_6\text{F}_5)]^+[\text{BBu}_n(\text{C}_6\text{F}_5)_{4-n}]^-$ was not observed. It apparently decomposes on formation via abstraction of a perfluorophenyl group from the borate anion to form $\text{B}(\text{C}_6\text{F}_5)_3$, $\text{Cp}_2\text{Zr}(\text{C}_6\text{F}_5)_2$, and other decomposition products. Although the other decomposition products were not identified, the $\text{Zr}(\text{C}_6\text{F}_5)$ fragment was detected in all of them. It is thus clear that the C_6F_5 group was not transferred from Zr to B in this case.

Reaction of $[\text{Cp}_2\text{Zr}(\text{C}_6\text{F}_5)(\mu\text{-H})_2]$ with $\text{B}(\text{C}_6\text{F}_5)_3$ did not result in transfer of C_6F_5^- to boron either. Instead, a relatively stable product, which NMR parameters suggest to be the starting molecule with a borane weakly coordinated to each of the bridging hydrides, was obtained. As judged by the ^1H chemical shift (-0.95 ppm) for the $\mu\text{-H}$ and the absence of a measurable H–B coupling (although the signal is significantly broadened by the B–H interaction), the Zr–H–Zr fragment is mainly preserved and any newly formed B–H bond is long and weak. However, the ^{19}F NMR spectrum exhibits a characteristic pattern for a tetracoordinated borate, which is very different from the spectrum of the starting tricoordinated borane. A minor decomposition occurred by the abstraction of a perfluorophenyl group from the borate anion, as was the case with cationic $[\text{Cp}_2\text{Zr}(\text{C}_6\text{F}_5)]^+[\text{BBu}_n(\text{C}_6\text{F}_5)_{4-n}]^-$. The low reactivity of the cationlike compound can be attributed to its dimeric structure. In an attempt to cleave the dimer, the reaction was repeated in THF. The main product was $\text{Cp}_2\text{Zr}(\text{C}_6\text{F}_5)(\text{OBU})$, which results from THF ring opening by the strongly acidic Zr center. No Zr to B ligand transfer was observed in this case either.

A similar reactivity pattern was reported by Marks and co-workers, who observed that ligand transfer is readily reversible when the group is Me but not when

(41) Cardin, D. J.; Lappert, M. F.; Raston, C. L. *Chemistry of Organo-Zirconium and -hafnium Compounds*; Ellis Horwood: Chichester, U.K., 1986.

(42) Seewald, P. A.; White, G. S.; Stephan, D. W. *Can. J. Chem.* **1988**, *66*, 1147–1152.

(43) Borkowsky, S. L.; Baenziger, N. C.; Jordan, R. F. *Organometallics* **1993**, *12*, 486–495.

(44) Merola, J. S.; Campo, K. S.; Gentile, R. A.; Modrick, M. A. *Inorg. Chim. Acta* **1989**, *165*, 87–90.

(45) Coutts, R. S. P.; Kautzner, B.; Wailes, P. C. *Aust. J. Chem.* **1969**, *22*, 1137–1141.

(46) Green, M. L. H.; Lucas, C. R. *J. Chem. Soc., Dalton Trans.* **1972**, 1000–1003.

(47) Samuel, E.; Vedel, J. *Organometallics* **1989**, *8*, 237–241.

(48) Lockhart, J. C. *Chem. Rev.* **1965**, *65*, 131–151.

(49) Siedle, A. R.; Newmark, R. A. *J. Organomet. Chem.* **1995**, *497*, 119–125.

(50) Aresta, M.; Quaranta, E.; Tommasi, I.; Derien, S.; Dunach, E. *Organometallics* **1995**, *14*, 3349–3356.

(51) de Rege, F. M. G.; Buchwald, S. L. *Tetrahedron* **1995**, *51*, 4291–4296.

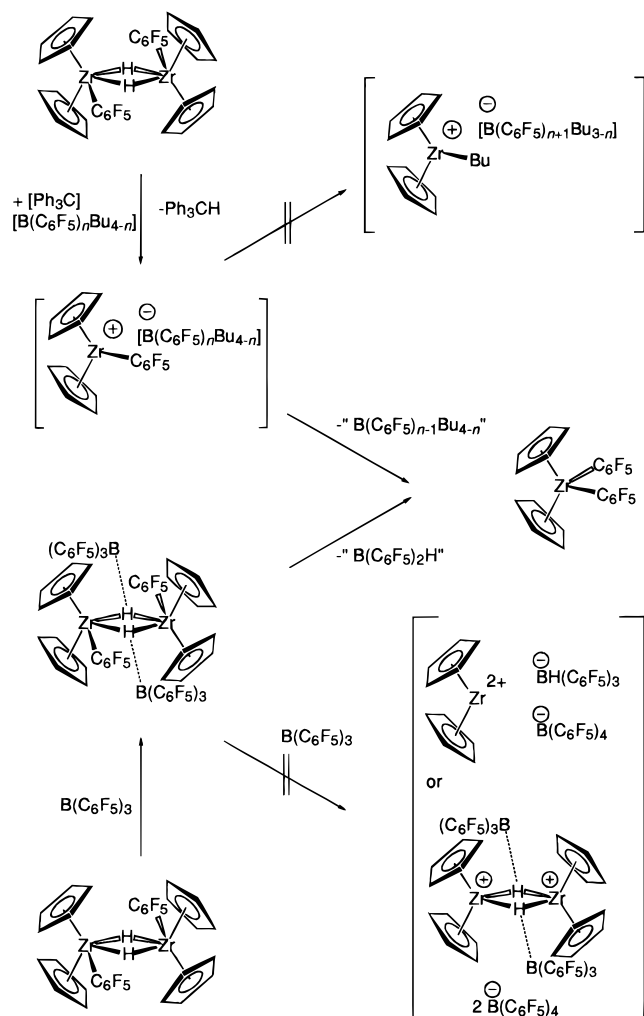
(52) Quintanilla, R.; Cole, T. E. *Tetrahedron* **1995**, *51*, 4297–4308.

(53) Marsella, J. A.; Caulton, K. G. *J. Am. Chem. Soc.* **1982**, *104*, 2361–2365.

(54) Siegmund, K.; Pregosin, P. S.; Venanzi, L. M. *Organometallics* **1989**, *8*, 2659–2664.

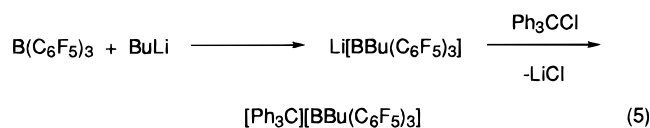
(55) Albano, P.; Aresta, M.; Manassero, M. *Inorg. Chem.* **1980**, *19*, 1069–1072.

Scheme 3. Attempted Pentafluorophenyl Group Transfer Reactions from Zirconium to Boron Nuclei



it is C_6F_5 .^{31,33} The above data strongly suggest that zirconium does not participate in the redistribution of the borate ligands in the present case. Besides, neither $Cp_2Zr(C_6F_5)^+$ nor $Cp_2Zr(C_6F_5)_2$ was detected among the products of eq 1.

To test the alternative pathway, a synthesis of $[Ph_3C][BBu(C_6F_5)_3]$ was attempted (eq 5). Interestingly, $[Ph_3C]$ -



$[BBu(C_6F_5)_3]$ is only present in substantial quantities in freshly prepared samples. $[Ph_3C][BBu_2(C_6F_5)_2]$ and $[Ph_3C][B(C_6F_5)_4]$, whose presence was confirmed by ^{19}F NMR spectroscopy, are formed quite rapidly upon storage of the solutions. The redistribution pathway can be analyzed by ^{19}F NOESY experiments. In some cases there is an extra set of ^{19}F NMR resonances in addition to the signals due to the bis-, tris-, and tetrakis-(pentafluorophenyl)borates (Figure 4). These peaks are in slow dynamic exchange with the $[Ph_3C][BBu_2(C_6F_5)_2]$ signals, as can be seen from the "out-of-phase" NOE peaks arising from the F nuclei of different borates. This indicates a slow intermolecular ligand exchange process

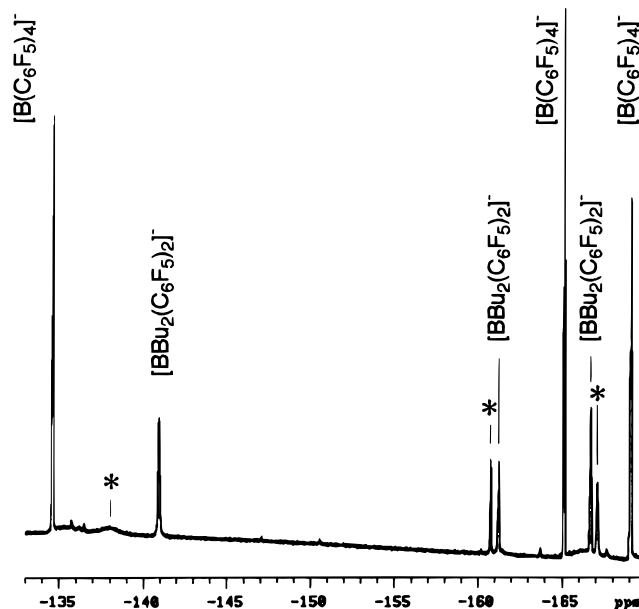


Figure 4. ^{19}F NMR spectrum of $[Ph_3C][BBu_n(C_6F_5)_{4-n}]$ in C_6D_6 . There is an extra set of ^{19}F NMR resonances, marked by asterisks, in addition to the signals due to $[Ph_3C][BBu_2(C_6F_5)_2]$ and $[Ph_3C][B(C_6F_5)_4]$, which is in slow dynamic exchange with the former.

(Scheme 2, path 1). The regular "in phase" intramolecular NOEs for the neighboring fluorine atoms within the C_6F_5 ring can be observed as well. This process is irreversible; it accelerates at elevated temperatures and stops when only $[Ph_3C][BBu_2(C_6F_5)_2]$ and $[Ph_3C][B(C_6F_5)_4]$ are present in the system. The extra set of ^{19}F NMR signals is not likely to belong to $[Ph_3C][BBu_3(C_6F_5)]$ in a degenerate exchange with $[Ph_3C][BBu_2(C_6F_5)_2]$, since there is no evidence of exchange with the other borates on the same time scale, nor are the other borates exchanging with each other. The most probable mechanism for the ligand redistribution is transfer between a tetracoordinate borate ion and a catalytic amount of a neutral borane. However, there is certainly not enough neutral borane present to account for the unassigned peaks. Although the origin of the unassigned resonances is unclear and the exact mechanism of the redistribution is unknown, the experiment clearly demonstrates that (perfluorophenyl)borates can and do undergo redistribution without any external assistance or catalysis from the zirconocene species.

III. Reactivity and Thermal and Photolytic Degradation of 1a. Marks and co-workers recently reported that some of the cationic zirconocenes with tetrakis(pentafluorophenyl)borate anions decompose at elevated temperatures by abstraction of fluoride or pentafluorophenyl by zirconium as well as by CH activation of the Cp ligand or aromatic hydrocarbon solvent, which precludes their use in high-temperature processes.³¹ The low stability was attributed to the cationic charge on zirconium and to an open coordination sphere. It was of interest to study the thermal stability of **1a**, which also contains similar borate anions but has the positive charge delocalized between Zr and Si.¹⁸ As a result of this charge delocalization **1a** proved to be much more thermally stable. At room temperature solid samples or solutions in hydrocarbon solvents have been stored for years in the absence of light

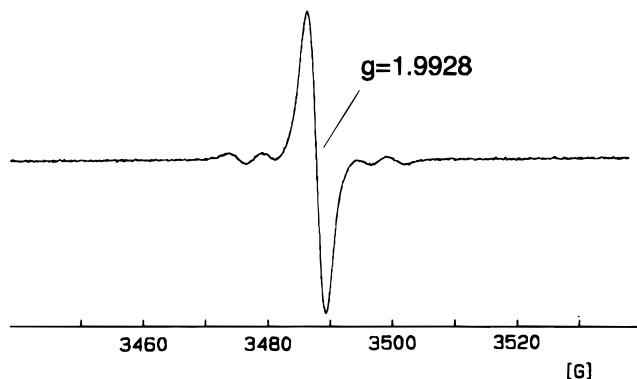
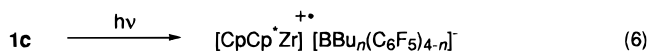


Figure 5. EPR spectrum of $[\text{CpCp}^*\text{Zr}][\text{BBu}_n(\text{C}_6\text{F}_5)_{4-n}]$ in toluene.

without noticeable decomposition. At higher temperatures (above $+60\text{ }^\circ\text{C}$) decomposition occurs in a matter of minutes, with the major pathway being the loss of the Bu group and formation of $\text{BH}_n(\text{C}_6\text{F}_5)_{4-n}$ anions.^{26,31} Prolonged heating caused pentafluorophenyl but not fluoride abstraction by zirconium and further decomposition to species which were not identified.

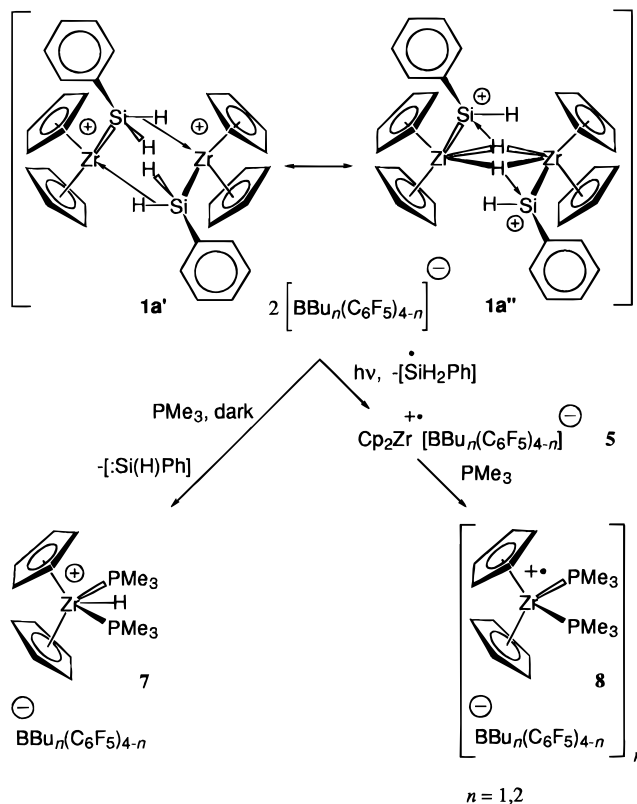
The same Bu–B decomposition reaction can also occur upon irradiation of the sample with a daylight fluorescent lamp. In addition, irradiation causes Zr(IV) to Zr(III) reduction accompanied by elimination of PhSiH_3 and formation of a number of radical species. The first EPR signal to appear upon irradiation is a broad and featureless singlet ($g = 2.0036$). Such a high g value cannot be due to a zirconocene. In view of this, and the absence of observable satellite peaks, this signal is tentatively attributed to a silicon-centered radical. A second EPR signal appears either simultaneously or shortly after the first one and grows at its expense in the dark. This signal is due to **5** ($g = 1.9964$, s , $a(\text{Zr}) = 7.1\text{ G}$), *vide supra*. It is gradually replaced by another peak, assigned in section II to an inner sphere solvated form of **5** ($g = 1.9972$, s , $a(\text{Zr}) = 12.3\text{ G}$). These redox transformations are reversible, and a slow reaction of silane with **5** regenerates **1a** when the sample is left in the dark for 1–2 months. It is of interest that similar spectral transformations have been reported for the $\text{Cp}_2\text{ZrCl}_2\text{--MAO}$ system.⁵⁶ A $\text{Cp}_2\text{Zr}(\mu\text{-Cl})_2\text{MAO}$ cationlike complex ($g = 1.998$, $a(\text{Zr}) = 7\text{ G}$) formed adducts with ethylene and styrene ($g = 1.998$, $a(\text{Zr}) = 12\text{ G}$ and $g = 1.998$, $a(\text{Zr}) = 13\text{ G}$, respectively). Although the changes in the $a(\text{Zr})$ value were attributed to the formation of a $\text{Cp}(\text{Cl})\text{Zr}(\mu\text{-Cl})_2\text{--MAO}$ complex,⁵⁶ an adduct with an olefin seems to be a more likely explanation, since such an olefin adduct accounts for the differences between the ethylene and styrene experiments.

$[\text{CpCp}^*\text{Zr}(\mu\text{-H})(\text{SiHPh})]_2^{2+}[\text{BBu}_n(\text{C}_6\text{F}_5)_{4-n}]_2^{2-}$ (**1c**) also undergoes photolytic decomposition (eq 6). In this case,



however, a single product is formed ($g_{\text{iso}} = 1.9928$ at room temperature, Figure 5, s , $a(\text{Zr}) = 5.1\text{ G}$; $g_x = 1.9915$, $g_y = 1.9845$, $g_z = 2.0060$ at $-150\text{ }^\circ\text{C}$). The difference between g_{iso} and the value of 1.9940 calculated for g_{av} together with the relatively high value of g_y indicates some π stabilization in this compound,

Scheme 4. Two Possible Routes of the PMe_3 -Assisted Zr–Si Bond Cleavage Reaction



although the effect is less pronounced than in **5**, as both $a(\text{Zr})$ and g_y are higher in the latter (*vide supra*). Such a stabilization can be attributed either to a cation–anion interaction, as discussed above, or to an agostic interaction between Zr and one of the Me groups of the Cp^* ligand, which blocks a coordination site and precludes tight coordination of toluene. Although formation of an insoluble clathrate of **1c** and its derivatives is observed under some conditions, it did not occur in the above-mentioned EPR sample, which remained homogeneous.

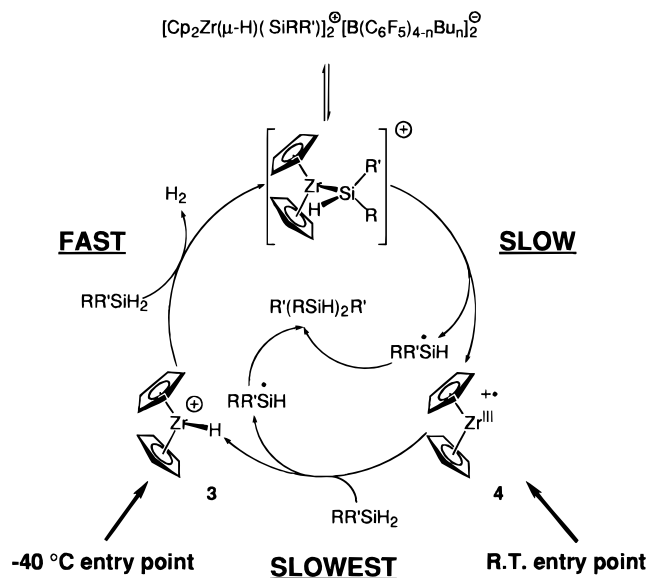
When a preirradiated sample of **1a** was treated with PMe_3 , all of the EPR signals described above disappeared (Scheme 4) and were replaced by a clean triplet assigned to **8** (*vide supra*). Quantitative measurement of the concentration of **8** from its EPR signal showed it to account for about 3% of the total Zr. The other product of this reaction exhibits broad and featureless ^1H NMR resonances in the Cp and PMe_3 regions, which precluded an accurate characterization. It is tentatively assigned as the dimer $[\text{Cp}_2\text{Zr}^{\text{III}}(\text{PMe}_3)_x]_2^{2+}[\text{BR}_n(\text{C}_6\text{F}_5)_{4-n}]_2^{2-}$ ($\text{R} = \text{Bu}, \text{H}$), the signals of which are broadened due to a fast exchange with its paramagnetic monomer **8**.

The reaction of **1a** with PMe_3 took a different course in the dark. The major product (up to 50%) of this reaction is **7**, not **8**. The latter is formed in only trace amounts (less than 1%).

IV. Mechanism of the $\text{Cp}_2\text{ZrCl}_2/\text{B}(\text{C}_6\text{F}_5)_3/\text{BuLi}$ Catalyzed Dehydropolymerization of Silanes. As mentioned above, the catalytic activity of the $\text{Cp}_2\text{ZrCl}_2/\text{B}(\text{C}_6\text{F}_5)_3/\text{BuLi}$ precatalyst is very dependent on the temperature of preparation. Catalysts prepared at low temperature are almost inactive, while those prepared at room temperature give high rates and polymers of

(56) Cam, D.; Sartori, F.; Maldotti, A. *Macromol. Chem. Phys.* **1994**, *195*, 2817–2826.

Scheme 5. Proposed Redox Mechanism for Reactions of Silanes with "cationlike" Silylzirconocenes (R = Ar, Alk; R' = H, (SiHR)_nH)



unusually high molecular weight. The main difference between the two temperature regimes is that at -40 °C the zirconocene does not undergo reduction, whereas at $+25$ °C it does. However, as shown in Scheme 1, and discussed in detail above, in the presence of PhSiH_3 both the Zr(IV) and Zr(III) species react to give the same products **4** and **6**. At first glance this presents a problem if one wishes to formulate a mechanism which involves one or both of these species. A possible resolution of this dilemma is illustrated in Scheme 5, which shows a catalytic cycle involving a combination of one-electron redox steps and a σ -bond metathesis step.

The key to a sustainable cycle is avoidance of the dimerization of the $[\text{Cp}_2\text{ZrSiH}_2\text{Ph}]^+$ species. The formation of the dimer **1** is thermally irreversible and represents a loss of active catalyst. (Note: the photochemical cleavage of this dimer, together with further evidence for the three steps of the cycle, is the subject of a following paper.) The rate of loss of $[\text{Cp}_2\text{ZrSiH}_2\text{Ph}]^+$ through dimerization is proportional to the square of its concentration, whereas its homolysis is first order. Hence, dimerization is favored at high concentrations of $[\text{Cp}_2\text{ZrSiH}_2\text{Ph}]^+$ and homolysis at low concentrations. The mechanism presented in Scheme 5 shows the two different points of entry into the catalytic cycle that are characteristic of the low-temperature and room-temperature protocols. The hierarchy of rates shown in this scheme for the three steps of the cycle leads to most of the zirconium being transformed to $[\text{Cp}_2\text{ZrSiH}_2\text{Ph}]^+$ if it enters the cycle as $[\text{Cp}_2\text{ZrH}]^+$, but most remaining as $[\text{Cp}_2\text{Zr}]^+$ if it enters as such.

If the difference between the low- and ambient-temperature protocols does not reside in a kinetic phenomenon, such as that described above, it must be concluded that the difference is due to a hitherto undetected intermediate.

Conclusions

The formation of $[\text{Cp}'_2\text{Zr}(\mu\text{-H})(\text{SiHR})]_2^{2+}[\text{BBu}_n(\text{C}_6\text{F}_5)_{4-n}]_2^{2-}$ ($\text{Cp}' = \text{Cp}, \text{MeCp}, \text{Me}_5\text{Cp}$; $\text{R} = \text{Ph}, \text{PhCH}_2$;

1a-d) from $\text{Cp}'_2\text{ZrCl}_2$, BuLi, $\text{B}(\text{C}_6\text{F}_5)_3$, and PhSiH_3 involves three distinct processes: (i) formation and decomposition of ZrBu compounds, (ii) transfer of Bu groups from Zr to B to produce borate anions, (iii) reaction of silane with Zr intermediates, and (iv) redistribution of Bu and C_6F_5 groups between borate anions.

At $-20/-40$ °C, processes i–iii occur by ligand substitution and constant oxidation σ -bond metatheses. At room temperature (i) leads to reduced Zr(III) species which react with silanes by a one-electron oxidation, atom transfer mechanism. Process iv occurs by a mechanism that does not involve zirconocene species.

Experimental Section

Materials and Methods. General experimental techniques and solvent purifications were described earlier.¹⁸ All operations were performed in Schlenk-type glassware on a dual-manifold Schlenk line, equipped with flexible stainless steel tubing, or in an argon-filled M. Braun Labmaster 130 glovebox (<0.05 ppm of H_2O). Argon was purchased from Matheson (prepurified for the glovebox and UHP for the vacuum line) and was used as received. Hydrocarbon solvents (protio and deuterio benzene and toluene, pentane, and hexanes) were dried and stored over Na/K alloy, benzophenone, and 18-crown-6 in Teflon-valved bulbs and were vacuum-transferred prior to use. THF was vacuum-transferred from sodium benzophenone ketyl. Halogenated solvents and silanes (1,1,2,2-tetrachloroethane-*d*₂, $\text{C}_6\text{F}_5\text{Br}$, PhSiH_3 , and $\text{PhCH}_2\text{-SiH}_3$) were degassed and stored over molecular sieves. $\text{Cp}_2\text{-ZrCl}_2$, $[\text{Cp}_2\text{Zr}(\text{H})\text{Cl}]_2$, $\text{Me}_5\text{C}_5\text{H}$, ZrCl_4 , C_6D_6 , C_7D_8 , 1,1,2,2-tetrachloroethane-*d*₂, $\text{C}_6\text{F}_5\text{Br}$, Ph_3CCl , $\text{PhC}(\text{O})\text{Ph}$, 18-crown-6, BCl_3 (1.0 M in heptane), *n*-BuLi (2.5 M in hexanes), PMe_3 (1.0 M in toluene), CpNa (2.0 M solution in THF), magnesium powder, and CDCl_3 were purchased from Aldrich and used as received unless stated otherwise.

The compounds $(\text{MeCp})_2\text{ZrCl}_2$,⁵⁷ $[(\text{MeCp})\text{Zr}(\mu\text{-H})\text{H}]_2$,⁵⁸ $\text{CpCp}^*\text{ZrCl}_2$,⁵⁹ $\text{Cp}_2\text{Zr}^{\text{II}}(\text{PMe}_3)_2$,⁶⁰ $\text{B}(\text{C}_6\text{F}_5)_3$,⁶¹ $[\text{Ph}_3\text{C}]^+[\text{B}(\text{C}_6\text{F}_5)_4]^-$,⁶² and RSiH_3 ($\text{R} = \text{Ph}, \text{PhCH}_2$)⁶³ were prepared according to literature procedures.

Physical and Analytical Measurements. NMR spectra were recorded on Varian Unity 500 (FT, 500 MHz for ^1H), Varian XL-200, and Varian Gemini-200 (FT, 200 MHz for ^1H) spectrometers. Chemical shifts for ^1H and ^{13}C spectra were referenced using internal solvent references and are reported relative to tetramethylsilane. ^{19}F and ^{31}P spectra were referenced to external CF_3COOH and PMe_3 samples, respectively. Quantitative NMR measurements were performed using residual solvent protons as internal references. EPR spectra were recorded on a Bruker ESP 300E (X-band) spectrometer and were referenced to external DPPH. Quantitative EPR measurements were performed with an external standard of TEMPO of known concentration. Mass spectra were recorded on a Kratos MS25RFA spectrometer equipped with a Kratos DS90 data system. Elemental analyses were performed by Oneida Research Services, Inc., Whitesboro, NY. The photochemical experiments were performed using a general purpose 9 W compact daylight fluorescent bulb (Syl-

(57) Samuel, E. *Bull. Soc. Chim. Fr.* **1966**, 3548–3564.

(58) Jones, S. B.; Petersen, J. L. *Inorg. Chem.* **1981**, *20*, 2889–2894.

(59) Wolczanski, P. T.; Bercaw, J. E. *Organometallics* **1982**, *1*, 793–799.

(60) Kool, L. B.; Rausch, M. D.; Alt, H. G.; Herberhold, M.; Honold, B.; Thewalt, U. *J. Organomet. Chem.* **1987**, *320*, 37–45.

(61) Massey, A. G.; Park, A. J. *J. Organomet. Chem.* **1964**, *2*, 245–250.

(62) Chien, J. C. W.; Tsai, W.-M.; Rausch, M. D. *J. Am. Chem. Soc.* **1991**, *113*, 8570–8571.

(63) Finholt, A. E.; Bond, A. C. J.; Wilzbach, K. E.; Schlesinger, H. I. *J. Am. Chem. Soc.* **1947**, *69*, 2692–2696.

vania, Model No. F9DTT/27K) with an output primarily in the 350–650 nm spectral region.⁶⁴

All NMR samples were prepared in an NMR-tube assembly, consisting of one or more 5 mL round-bottom flasks fitted with a Teflon valve to which an NMR tube was fused at an angle of 45°. Components of an NMR sample were loaded separately, when necessary, in each of the flasks and were mixed in appropriate order by transferring from one flask of choice to the other by tilting of the entire apparatus. A sample was treated with small quantities (0.1–0.2 mL) of a deuterated solvent of choice. The solvent was then evaporated and the evaporation–vacuum-transfer cycle was repeated to remove any residual nondeuterated solvent. A fresh portion of the same deuterated solvent (0.6–0.7 mL) was then vacuum-transferred into the assembly, and the solution was carefully decanted into the side NMR tube. The top part of the tube was washed by touching it with a swab of cotton wool soaked with liquid nitrogen, which causes condensation of the solvent vapors on the inner walls. The sample was then frozen and flame-sealed.

Low-Temperature Reaction of Cp₂ZrBu₂ with B(C₆F₅)₃. Cp₂ZrCl₂ (0.073 g, 0.25 mmol), (C₆F₅)₃B (0.128 g, 0.25 mmol), and a 2.5 M solution of BuLi in hexanes (0.2 mL, 0.50 mmol) were loaded in separate flasks of a triple-flask NMR assembly (*vide supra*). The flask with BuLi was isolated from the rest of the assembly by a Teflon valve, and the hexanes were removed under vacuum. Toluene-*d*₈ was then vacuum-transferred into that flask (0.1–0.2 mL). The evaporation–vacuum-transfer cycle was repeated twice to remove any residual hexanes, and a final fresh portion of toluene-*d*₈ (0.8–1 mL) was vacuum-transferred into the assembly. The entire apparatus was then immersed in a CH₃CN–dry ice bath (–41 °C), and the solution of BuLi was mixed with Cp₂ZrCl₂. The mixture was stirred at –41 °C for 1 h, and the cold yellow solution was then mixed with (C₆F₅)₃B and stirred for another 30 min at –41 °C. A brownish yellow oil was formed almost instantaneously. The residue was allowed to settle for 30 min at –41 °C and the mother liquor was decanted from the precipitated LiCl into the NMR tube. The sample was frozen and flame-sealed under vacuum.

[Cp₂ZrBu]⁺[BBu_{*n*}(C₆F₅)_{4–*n*}][–] data are as follows: NMR (C₇D₈, –20 °C): ¹H δ 5.69 (s, Cp), 1.82 (m, α-BuB), 1.68 (m, γ-BuB), 1.40 (m, β-BuZr), 1.35 (m, γ-BuZr), 1.32 (m, β-BuB), 1.06 (t, δ-BuB), 0.86 (masked by BuH peak, δ-BuZr), 0.38 (m, α-BuZr); ¹³C (from ¹H–¹³C HMQC) δ 113.2 (Cp), 50.8 (α-BuZr), 36.1 (β-BuZr), 31.5 (β-BuB), 27.4 (γ-BuB), 24.1 (γ-BuZr), 23.7 (α-BuB), 14.3 (δ-BuB), 11.6 (δ-BuZr); ¹⁹F δ [BBu₂(C₆F₅)₂][–] –139.9 (br s, *o*-C₆F₅), –161.3 (br s, *p*-C₆F₅), –165.7 (br s, *m*-C₆F₅); ¹⁹F δ [BBu(C₆F₅)₃][–] –137.9 (br s, *o*-C₆F₅), –163.7 (br s, *p*-C₆F₅), –166.6 (br s, *m*-C₆F₅). The resonances of residual Cp₂ZrBu₂²⁴ (ca. 5% of the observable Cp signals) and butane are not listed.

Quenching the Cp₂ZrBu₂/B(C₆F₅)₃/PhSiH₃ Mixture with PMe₃. A mixture of Cp₂ZrBu₂ and B(C₆F₅)₃ (0.25 mmol) was prepared in toluene as described above. PhSiH₃ (0.13 mL, 1.0 mmol) was then added, and stirring was continued for a further 2 h while the solution was warmed gradually to 0 °C. A 1.0 M toluene solution of PMe₃ (1.0 mL, 1.0 mmol) was added. The mixture was stirred for 1 h, and an NMR/EPR sample was prepared as described above.

[Cp₂ZrH(PMe₃)₂]⁺[BBu_{*n*}(C₆F₅)_{4–*n*}][–] data are as follows: NMR (C₆D₆, 25 °C): ¹H δ 4.88 (t, *J*_{HP} = 2.3 Hz, Cp), 2.05 (m, α-Bu), 1.78 (q, γ-Bu), 1.57 (m, β-Bu), 1.12 (t, ²*J*_{HH} = 7.4 Hz, δ-Bu), 0.66 (t, ²*J*_{HP} = 104.1 Hz, HZr), 0.60 (equal intensity t, *J*_{HP} = 4.0 Hz, Me₃P); ¹³C δ 101.7 (Cp), 17.8 (Me₃P); ³¹P δ 0.8 (104 Hz, Me₃P) (approximately 60% of the overall amount of [BBu]).

[Cp₂Zr^{III}(PMe₃)₂]⁺[BBu_{*n*}(C₆F₅)_{4–*n*}][–] data are as follows: NMR (C₆D₆, 25 °C): ¹H δ 2.05 (m, α-Bu), 1.78 (q, γ-Bu), 1.57 (m, β-Bu), 1.12 (t, ²*J*_{HH} = 7.4 Hz, δ-Bu). EPR (C₆D₆, 25 °C): *g* = 1.9877 (t, *a*(P) = 33.0 G, *a*(Zr) = 23.4 G).

Reaction of Cp₂ZrBu with B(C₆F₅)₃. Cp₂ZrBu was synthesized from Cp₂ZrCl₂ (0.0365 g, 0.125 mmol) and BuLi (0.1 mL of 2.5 M solution in hexanes, 0.25 mmol) in 5 mL of toluene (1 day at room temperature).²⁴ (C₆F₅)₃B (0.064 g, 0.125 mmol) was added, and an EPR sample was frozen and flame-sealed under vacuum.

EPR (toluene, +25 °C): *g* = 1.9964 (br s, *a*(Zr) = 7.1 G), *g* = 1.9972 (s, *a*(Zr) = 12.3 G).

Reaction of Cp₂ZrBu with [Ph₃C]⁺[BBu_{*n*}(C₆F₅)_{4–*n*}][–] (Average *n* = 1). Cp₂ZrBu (0.125 mmol) was synthesized in 5 mL of toluene as described above. [Ph₃C]⁺[BBu_{*n*}(C₆F₅)_{4–*n*}][–] (0.101 g, 0.125 mmol) was added and the mixture stirred for 5 min. The color changed from brown-red to light yellow. An EPR sample was frozen and flame-sealed under vacuum.

EPR (toluene, +25 °C): Ph₃C[•], *g* = 2.0021 (m); poorly resolved 5, *g* = 1.9972 (s, *a*(Zr) = 12.3 G).

Thermal Degradation of 2. An EPR sample of Cp₂ZrBu₂–B(C₆F₅)₃ was prepared as described above in toluene. The sample was warmed to room temperature, while the changes were monitored by EPR.

Early decomposition stage (1–30 min): EPR (toluene, +25 °C) *g* = 1.9860 (s, *a*(Zr) = 25.8 G), *g* = 1.9964 (br s, *a*(Zr) = 7.1 G), *g* = 1.9972 (s, *a*(Zr) = 12.3 G).

Late decomposition stage (1–30 days), EPR (toluene, +25 °C) *g*_{iso} = 1.9972 (s, *a*(Zr) = 12.3 G); EPR (toluene, –150 °C) *g*_x = 1.9970, *g*_y = 1.9900, *g*_z = 2.0075.

Reaction of [Cp₂Zr^{III}]⁺[BBu_{*n*}(C₆F₅)_{4–*n*}][–] with PhSiH₃.¹⁸ Cp₂ZrCl₂ (0.219 g, 0.75 mmol) and (C₆F₅)₃B (0.384 g, 0.75 mmol) were loaded into separate Schlenk tubes in the glove-box. Toluene was vacuum-transferred into both tubes (8 mL each). The Cp₂ZrCl₂ was suspended in toluene at –41 °C (CH₃CN–dry ice bath), and a 2.5 M solution of BuLi in hexanes (0.6 mL, 1.50 mmol) was added. The mixture was stirred at room temperature for 1 h. The color changed from white to brown. The toluene solution of (C₆F₅)₃B was transferred by cannula into the butylated zirconocene solution. A brown-red oil was formed almost instantaneously. The reaction mixture was protected from light with aluminum foil and was stirred for 1 h. PhSiH₃ (0.56 mL, 4.50 mmol) was then added, and the stirring was continued for a further 3 h. The solvent was partially evaporated (leaving 1–2 mL), and pentane was vacuum-transferred into the tube, causing precipitation of a purple slurry. The brown mother liquor was removed, and the residue was washed with two additional portions of pentane (2 × 10 mL) and dried under vacuum to furnish a microcrystalline powder. The product was dark purple and mainly contained **1a**, contaminated by polyphenylsilane and traces of highly colored, unidentified, zirconocene compounds (crude yield ~75%).

[Cp₂Zr^{III}(PMe₃)₂]⁺[BBu_{*n*}(C₆F₅)_{4–*n*}][–] (**8**). Cp₂ZrBu (0.75 mmol) was synthesized in 10 mL of toluene as described above. A solution of (C₆F₅)₃B (0.384 g, 0.75 mmol) in 10 mL of toluene was added via syringe, and the mixture was stirred for 1 h. A 1.0 M toluene solution of PMe₃ (2.0 mL, 2.0 mmol) was added, and the sample was used for EPR analysis without further purification.

EPR (toluene, +25 °C): *g* = 1.9877 (t; *a*(P) = 33.0 G, *a*(Zr) = 23.4 G).

Reaction of Cp₂Zr^{III}(PMe₃)₂ with [Ph₃C]⁺[BBu_{*n*}(C₆F₅)_{4–*n*}][–] (Average *n* = 1). A mixture of Cp₂Zr^{III}(PMe₃)₂ (0.0187 g, 0.05 mmol) and [Ph₃C]⁺[BBu_{*n*}(C₆F₅)_{4–*n*}][–] (0.0812 g, 0.10 mmol) was stirred for 5 min in toluene, and the solution was decanted into an EPR tube.

EPR (toluene, +25 °C): Ph₃C[•], *g* = 2.0021 (m); **8**.

[Ph₃C]⁺[BBu_{*n*}(C₆F₅)_{4–*n*}][–] (Average *n* = 1). In the glove-box, toluene (0.5 mL), (C₆F₅)₃B (0.128 g, 0.25 mmol), and a 2.5 M solution of BuLi in hexanes (0.100 mL, 0.25 mmol) were loaded in a Schlenk tube. A white precipitate was formed, and the mixture was stirred for 1 h. Ph₃CCl (0.077 g, 0.0275 mmol) was then added, and the reaction was continued for another 1 h. The mother liquor was transferred to the NMR assembly, and the product was precipitated upon addition of

(64) Rabek, J. F. *Experimental Methods in Photochemistry and Photophysics*; Wiley: Chichester, U.K., 1982, p 55.

pentane (3 mL). The supernatant was removed by syringe, and the red-brown solid was collected and washed with two portions of pentane (2 × 2 mL). An NMR sample was prepared in benzene-*d*₆.

NMR (C₆D₆, +25 °C): ¹H δ 7.35 (m, Ph), 7.06 (m, Ph), 6.98 (m, Ph).

NMR (C₆D₆, +25 °C) for [Ph₃C]⁺[B(C₆F₅)₄]⁻: ¹⁹F δ -134.6 (br s, *o*-C₆F₅), -165.1 (t, 21.4 Hz, *p*-C₆F₅), -169.1 (t, 17.4 Hz, *m*-C₆F₅); ¹³C δ 148.5 (*o*-C₆F₅), 136.4 (*m*-C₆F₅), 138.4 (*p*-C₆F₅) (ca. 30 mol % in a freshly prepared sample).

NMR (C₆D₆, +25 °C) for [Ph₃C]⁺[BBu(C₆F₅)₃]⁻: ¹⁹F δ -135.3 (br s, *o*-C₆F₅), -163.5 (t, 20.7 Hz, *p*-C₆F₅), -166.4 (br s, *m*-C₆F₅) (ca. 40 mol % in a freshly prepared sample).

NMR (C₆D₆, +25 °C) for [Ph₃C]⁺[BBu₂(C₆F₅)₂]⁻: ¹⁹F δ -140.9 (br s, *o*-C₆F₅), -161.2 (t, 19.8 Hz, *p*-C₆F₅), -166.7 (t, 19.0 Hz, *m*-C₆F₅) (ca. 30 mol % in a freshly prepared sample).

When the reaction mixture of (C₆F₅)₃B with BuLi was stirred for 2 days prior to introduction of Ph₃CCl, an unassigned set of peaks was observed. ¹⁹F NMR: δ -138.0 (br s, *o*-[B(C₆F₅)₃]⁻), -160.8 (t, 20.7 Hz, *p*-[B(C₆F₅)₃]⁻), -167.1 (br s, *m*-[B(C₆F₅)₃]⁻) (ca. 20 mol % in a sample immediately following addition of Ph₃CCl).

Cp₂Zr(C₆F₅)₂. This procedure differs from that reported by Chaudhari and Stone⁶⁵ in that a Grignard reagent was used instead of aryllithium. Mg powder (0.097 g, 4.00 mmol) was loaded in a Schlenk flask and was dried under vacuum at 60 °C. THF (15 mL) was vacuum-transferred into the flask, and C₆F₅Br (0.50 mL, 4 mmol) was added to the cooled (-78 °C) suspension. The reaction mixture was warmed gradually and was stirred for 6 h at room temperature. The color of the mixture changed from colorless to light yellow and then brownish as soon as the solution reached room temperature. The solution was recooled (-78 °C) and transferred via cannula to a Schlenk flask containing Cp₂ZrCl₂ (0.526 g, 1.8 mmol). The reaction mixture was stirred for 24 h at room temperature to give a dark green solution. The solvent was evaporated, and the residue was redissolved in toluene (25 mL) and recrystallized from toluene/pentane (25 mL/25 mL). A greenish white solid was collected by filtration and sublimed at 120–150 °C/0.01–0.001 Torr to furnish white crystalline product: yield 0.320 g, 46%.

NMR (C₆D₆, +25 °C): ¹H δ 5.72 (s, Cp); ¹⁹F δ -120.5 (br s, *o*-C₆F₅), -157.8 (t, 19.9 Hz, *p*-C₆F₅), -164.5 (m, *m*-C₆F₅); ¹³C δ 136.5 (*m*-C₆F₅), 139.8 (*p*-C₆F₅). MS (EI, ion source 200 °C, 70 eV, direct inlet 100 °C; *m/z* (relative intensity)): 554 (M⁺, 15), 239 (25), 220 (20), 193 (45), 175 (40), 168 (100).

[Cp₂Zr(C₆F₅)(μ-H)]₂. Mg powder (0.049 g, 2.00 mmol) was loaded in a Schlenk flask and was dried under vacuum at 60 °C. THF (15 mL) was vacuum-transferred into the flask, and C₆F₅Br (0.25 mL, 2 mmol) was added to the cooled (-78 °C) suspension. The reaction mixture was warmed gradually and was stirred for 3 h at room temperature. The color of the mixture changed from colorless to light yellow and then brownish as soon as the solution reached room temperature. The cold (-78 °C) solution was transferred via cannula to a Schlenk flask containing Cp₂Zr(H)Cl (0.468 g, 1.8 mmol), and the reaction mixture was stirred for 24 h at room temperature. The mother liquor was then removed, and the residue was redissolved in hot THF (35 mL). Hot toluene (15 mL) was added, and the mixture cooled to room temperature. A white crystalline product was collected by filtration, washed with pentane, and dried under vacuum: yield 64%. Anal. Calcd for C₁₆H₁₁F₅Zr: C, 49.34; H, 2.85. Found: C, 49.16; H, 2.74.

NMR (C₆D₆, +25 °C): ¹H δ 5.59 (s, Cp), -1.92 (q, 6.5 Hz, μ-H); ¹⁹F δ -107.0 (d, 27.3 Hz, *o*-C₆F₅), -160.8 (t, 19.8 Hz, *p*-C₆F₅), -164.7 (t, 19.8 Hz, *m*-C₆F₅).

Reaction of [Cp₂Zr(C₆F₅)(μ-H)]₂ with B(C₆F₅)₃ in C₆D₆. In the glovebox, [Cp₂Zr(C₆F₅)H]₂ (0.008 g, 0.01 mmol), B(C₆F₅)₃ (0.010 g, 0.02 mmol), and C₆D₆ were loaded in an NMR tube

assembly (*vide supra*). The sample was then frozen and flame-sealed. Cp₂Zr(C₆F₅)₂ was identified by a comparison to an authentic sample (*vide supra*). The estimated yields, by integration of the Cp peaks, of [Cp₂Zr(C₆F₅)(μ₃-HB(C₆F₅)₃)]₂ and Cp₂Zr(C₆F₅)₂ are 95 and 4%, respectively.

[Cp₂Zr(C₆F₅)(μ₃-HB(C₆F₅)₃)]₂ data are as follows: NMR (C₆D₆, +25 °C): ¹H δ 5.49 (s, Cp), -0.95 (br s, μ-H); ¹³C δ 148.2 (*o*-BH(C₆F₅)₃⁻), 146.6 (*o*-Zr(C₆F₅)), 140.5 (*p*-BH(C₆F₅)₃⁻), 140.2 (*p*-Zr(C₆F₅)), 137.6 (*m*-BH(C₆F₅)₃⁻), 137.4 (*m*-Zr(C₆F₅)), 114.7 (Cp); ¹⁹F δ -164.9 (t, 22.8 Hz, *m*-BH(C₆F₅)₃⁻), -163.5 (m, *m*-Zr(C₆F₅)), -157.2 (t, 21.4 Hz, *p*-BH(C₆F₅)₃⁻), -156.8 (t, 20.0 Hz, *p*-Zr(C₆F₅)), -137.1 (br s, *o*-BH(C₆F₅)₃⁻), -114.0 (br s, *o*-Zr(C₆F₅)).

Reaction of [Cp₂Zr(C₆F₅)(μ-H)]₂ with B(C₆F₅)₃ in THF. In the glovebox, [Cp₂Zr(C₆F₅)H]₂ (0.008 g, 0.01 mmol) and B(C₆F₅)₃ (0.010 g, 0.02 mmol) were loaded in an NMR tube assembly (*vide supra*). THF (5 mL) was vacuum-transferred into the assembly, and the reaction mixture was stirred for 2 h at room temperature. The solvent was removed under vacuum, and an NMR sample was prepared as described above.

Cp₂Zr(C₆F₅)(OBU) data are as follows: NMR (C₆D₆, +25 °C): ¹H δ 5.74 (s, Cp), 3.87 (t, 6.5 Hz, α-OBu), 1.33 (quintet, 7.0 Hz, β-OBu), 1.22 (sextet, 7.7 Hz, γ-OBu), 0.89 (t, 7.5 Hz, δ-OBu); ¹³C δ 111.2 (Cp), 75.2 (α-OBu), 22.5 (γ-OBu), 17.9 (β-OBu), 13.1 (δ-OBu); ¹⁹F δ -114.0 (br s, *o*-C₆F₅), -159.9 (t, 19.8 Hz, *p*-C₆F₅), -165.3 (t, 19.8 Hz, *m*-C₆F₅).

Reaction of [Cp₂Zr(C₆F₅)(μ-H)]₂ with [Ph₃C]⁺[BBu_{*n*}(C₆F₅)_{4-*n*}]⁻. In the glovebox, [Cp₂Zr(C₆F₅)H]₂ (0.008 g, 0.01 mmol), [Ph₃C]⁺[BBu_{*n*}(C₆F₅)_{4-*n*}]⁻ (average *n* = 1) (0.017 g, 0.03 mmol), and C₆D₆ were loaded in an NMR tube, and the sample was sealed with a rubber septum. The NMR tube was stored in an argon-filled container, and all NMR measurements were done within 1 h after the sample was removed from the container. The products were identified by a comparison to authentic samples of [Ph₃C]⁺[BBu_{*n*}(C₆F₅)_{4-*n*}]⁻ and B(C₆F₅)₃.

B(C₆F₅)₃ data are as follows: NMR (C₆D₆, +25 °C) ¹⁹F δ -131.5 (br s, *o*-C₆F₅), -144.2 (br s, *p*-C₆F₅), -162.6 (br s, *m*-C₆F₅); ¹³C δ 148.4 (*o*-C₆F₅), 145.2 (*p*-C₆F₅), 137.7 (*m*-C₆F₅).

Thermal Degradation of 1a. A sample of 1a in C₆D₆ was flame-sealed in an NMR tube which was kept at +60 °C for 4 h. The light yellow solution turned red-brown and deposited an oily precipitate. The [BH(C₆F₅)₃]⁻ moiety was identified by comparison to an independently synthesized sample of 1e.¹⁸

Photolytic Degradation of 1a. A sample of 1a in C₆D₆ was flame-sealed in an NMR tube and exposed to a daylight fluorescent lamp for 7 days. The light yellow solution turned red-brown and deposited an oily solid.

NMR (C₆D₆, +25 °C): ¹H δ 7.40–7.00 (m, PhSiH₃), 5.90 (br s, Cp), 4.22 (s, PhSiH₃), 1.88 (equal intensity quadruplet, ¹J_{BH} = 85 Hz), 1.20 (m, β-BuH), 0.85 (t, α-BuH). EPR (C₆D₆, +25 °C): *g* = 1.9964 (br s, *a*(Zr) = 7.1 G), *g* = 1.9972 (s, *a*(Zr) = 12.3 G), *g* = 2.0036 (br s).

Photolytic Degradation of 1c. A sample of 1c in toluene was flame-sealed in an NMR tube, which was exposed to a daylight fluorescent lamp for 5 min. The light yellow solution turned purple, but no precipitation occurred.

EPR (toluene, +25 °C): *g*_{iso} = 1.9925 (s, *a*(Zr) = 5.1 G). EPR (toluene, -150 °C): *g*_x = 1.9915, *g*_y = 1.9845, *g*_z = 2.0060.

Reaction of 1a with PMe₃. Dark Reaction. 1a (0.009 g, 0.005 mmol) was loaded in an NMR assembly. The reaction mixture was protected from light with aluminum foil. Whenever manipulations required removal of the protective foil, the lights in the laboratory were switched off. Toluene was then vacuum-transferred (1 mL), and a 1.0 M toluene solution of PMe₃ (0.050 mL, 0.05 mmol) was added. The mixture was stirred for 24 h, but no visible changes occurred. An NMR/EPR sample was prepared as described above.

[Cp₂ZrH(PMe₃)₂]⁺[BBu_{*n*}(C₆F₅)_{4-*n*}]⁻: concentration 0.005 M (approximately 50% of the starting [Zr]). The rest of the products (another 50% of the starting [BBu]) also contained the [BBu_{*n*}(C₆F₅)_{4-*n*}]⁻ moiety.

(65) Chaudhari, M. A.; Stone, F. G. A. *J. Chem. Soc. A* **1966**, 838–841.

Quantitative EPR measurements were always performed on a freshly prepared sample. A number of experiments were done with different acquisition parameters (modulation and microwave power) to ensure that there was no saturation of the signal. The other acquisition parameters were compensated for by a system normalization constant and were usually kept constant for both the unknown and the standard sample measurements.

$[\text{Cp}_2\text{Zr}^{\text{III}}(\text{PMe}_3)_2]^+[\text{BBu}_n(\text{C}_6\text{F}_5)_{4-n}]^-$: concentration 0.000 06 M (less than 1% of the starting [Zr]).

Photoreaction. **1a** (0.009 g, 0.005 mmol) was loaded in an NMR assembly. Toluene was then vacuum-transferred (1 mL), and the reaction mixture was irradiated with a 9 W daylight fluorescent light for 24 h. This was accompanied by a color change of the mixture from yellow to dark brown. A 1.0 M toluene solution of PMe_3 (0.050 mL, 0.05 mmol) was added, and the mixture was stirred for 24 h in the dark. An NMR/EPR sample was prepared as described above. The Cp and PMe_3 signals of $[\text{Cp}_2\text{ZrH}(\text{PMe}_3)_2]^+[\text{BBu}_n(\text{C}_6\text{F}_5)_{4-n}]^-$ were

detected but constituted less than 1% of the starting [Zr]. The rest of the resonances were lost in broad featureless bands at 6.4–5.2 and 1.4–0.2 ppm. The overall detectable concentration of $[\text{BBu}_n(\text{C}_6\text{F}_5)_{4-n}]^-$ was less than 1% of the starting [BBu].

$[\text{Cp}_2\text{Zr}(\text{PMe}_3)_2]^+[\text{BH}_n(\text{C}_6\text{F}_5)_{4-n}]^-$ data are as follows: EPR (C_6D_6 , 25 °C): $g = 1.9886$ (t, $a(\text{P}) = 33.2$ G, $a(\text{Zr}) = 23.4$ G). Concentration: 0.00025 M (approximately 3% of the starting [Zr]).

Acknowledgment. Financial support for this work from the NSERC of Canada and Fonds FCAR du Québec is gratefully acknowledged.

Supporting Information Available: NMR spectra (10 pages). Ordering information is given on any current masthead page.

OM960884O